Croatian Society for Materials Protection

Metalurgija/Metallurgy

Vol. 65 No. 3 / 2026

Effect of Tempering Temperature on Microstructure and Properties of 65Mn Spring Steel for Track and Field Starter

Haiyan Ma [1], Tong Tong [2,*], Heyu Shi [3] and Baihang Wang [4]

https://doi.org/10.64486/m.65.3.7

[1] Jinlin Sport University, No. 5699 Linhe Street, Economic Development Zone, Changchun City, Jilin Province, China, 130022; 0307@jlsu.edu.cn
[2] Changchun Normal University, No. 677, Changji North Line, Erdao District, Changchun City, Jilin Province, China, 130032; 65C10806110@365.udru.ac.th
[3] Changchun Automobile Economic and Technological Development Zone Sixth Middle School, No. 1751 Zhinong Street, Lvyuan District, Changchun City, Jilin Province, China, 130000; 67C10806126@365.udru.ac.th
[4] Udon Thani Rajabhat University, Ulongtani, Thailand, 10100; 66C10806110@365.udru.ac.th
* Correspondence: 65C10806110@365.udru.ac.th

Type of the Paper: Article
Received: September 4, 2025
Accepted: January 7, 2026

Abstract: 65Mn spring steel is a candidate material for elastic components in track and field starters due to its favorable combination of strength and elasticity. To optimize its performance for this demanding application, this work investigates the influence of tempering temperature on its mechanical properties and microstructure. The microstructure, hardness and tensile properties of the experimental spring steel after different tempering temperatures were studied. The effect of tempering temperature on the microstructure, hardness, strength, elongation and reduction of area of the alloy was clarified. The results indicate that a tempering temperature of 250 °C yields the optimal mechanical property profile, with a peak hardness of 631 HV, tensile strength of 2030.5 MPa, section shrinkage of 36.1 %, and elongation of 14.9 %. This combination of properties is deemed most suitable for application in track and field starters. This work provides a clear optimization of tempering parameters for this specific application, which has not been systematically reported in previous studies.

Keywords: track and field starter; 65Mn spring steel; microstructure; mechanical properties

1. Introduction

The track and field starter is a crucial piece of equipment in sprint events, directly influencing an athlete's starting efficiency and safety [1]. Its primary function is to provide a stable, anti-slip platform that allows the athlete to generate maximal horizontal force during the push-off phase. The biomechanics of sprint starts place unique demands on the starter's components, particularly the pedal and its support structure, which must withstand high impact loads, exhibit minimal permanent deformation over thousands of cycles, and provide consistent energy return [2, 3]. By providing a stable and adjustable platform, it optimizes starting posture, enhances biomechanical efficiency during the initial push-off phase, and helps convert physical potential into forward momentum more effectively [2].

Features such as anti-slip pedals and adjustable mechanisms also mitigate injury risks like ankle sprains caused by unstable footing [3–5]. Structurally, the device comprises a stable base, an adjustable mechanism for

personalized pedal positioning, and the pedals themselves. The elastic components within the pedal assembly are critical; they must absorb shock, reduce vibration transmitted to the athlete, and quickly return to their original shape. The pedal material's properties are critical, directly affecting force feedback and energy return. Advanced models may integrate sensors for performance monitoring. Spring steels are typically employed for components undergoing cyclic elastic deformation, such as the pedal support or return mechanism in a starter. 65Mn spring steel is widely used due to its excellent comprehensive mechanical properties, including high strength [6–8], good elasticity [9–11], and toughness [12–14]. Its composition, with ~0.65 % C and (0.90–1.20) % Mn, ensures good hardenability and strength, while manganese contributes to austenite stability and grain refinement, enhancing toughness and fatigue resistance [15–18]. This allows the material to maintain performance under repeated loading, extending equipment life and safety. Therefore, achieving the ideal balance of properties for a starter component namely, very high yield strength to prevent plastic deformation, sufficient toughness to avoid brittle fracture under impact, and good fatigue resistance is highly sensitive to the post-quench tempering process. However, its final properties are highly dependent on heat treatment processes like quenching and tempering, which control microstructure and optimize strength, hardness, and ductility [19–20].

While heat treatment of 65Mn steel has been studied, research targeting the specific property balance needed for track and field starter components—simultaneously high strength, good elasticity, and adequate toughness—is lacking. Previous studies have often focused on wear resistance [9], bending properties [10], or general mechanical trends [12, 15], but not on the precise tempering window that maximizes the synergistic combination of properties required for this specific sports engineering application. This study aims to fill this gap by systematically examining how tempering temperature affects the microstructure and mechanical properties of 65Mn spring steel, with the goal of identifying the optimal tempering process for this application.

2. Experimental conditions and methods

2.1. Experimental materials

The experimental material is 65Mn spring steel. This steel is widely used in China, with high strength, low decarburization tendency and good hardenability. Among them, the addition of Mn element improves the hardenability, so that after heat treatment and cold drawing hardening, the comprehensive mechanical properties are better than those of carbon steel while maintaining high strength and certain toughness and plasticity, and the cost is low. The chemical composition (mass fraction, %) of the steel is: C 0.65, Si 0.25, Mn 1.05, P $\leqslant$ 0.030, S $\leqslant$ 0.025, Cr $\leqslant$ 0.25, Ni $\leqslant$ 0.25, Cu $\leqslant$ 0.25, Fe balance. According to the continuous cooling transformation curve of 65Mn steel (Figure 1.), the supercooled austenite undergoes corresponding microstructure transformation at different temperatures and cooling rates: when the temperature is higher than about 430 °C and the cooling rate is lower than the critical cooling rate (about 20 °C / s), the supercooled austenite will be transformed into different forms of pearlite [48].

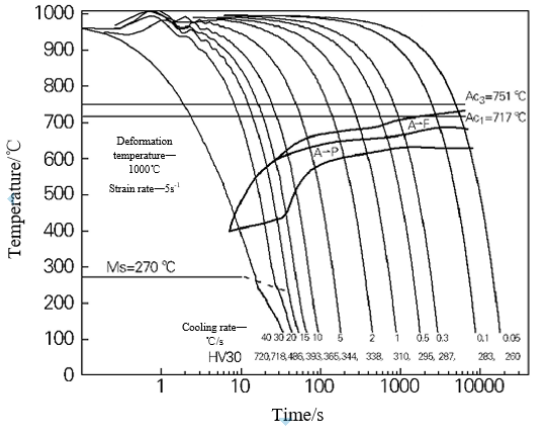

Figure 1. CCT curve of 65Mn steel

 https://doi.org/10.64486/m.65.3.7

From 430 °C to martensite start transition temperature (Ms), the undercooled austenite is in metastable state, and bainite transformation occurs during continuous cooling. When cooled below the Ms point, the supercooled austenite transforms into martensite. The critical temperatures of phase transformation of this steel are as follows: Ac1≈717 °C, Ac3≈751 °C, Ar1≈689 °C, Ar3 ≈741 °C, Ms≈270 °C.

2.2. Determination of mechanical properties

The mechanical properties of materials refer to the response characteristics of materials under external loads (such as tension, compression, bending, torsion, impact and alternating stress, etc.) in a specific environment. Generally, the mechanical properties of metal materials mainly include strength, plasticity, hardness, toughness, fatigue strength, elasticity and ductility.

In this study, the mechanical properties of 65Mn spring steel wire were systematically evaluated by hardness test, tensile test, torsion test, bending test and winding test.

2.2.1. Hardness test

The hardness test was carried out by Vickers hardness method. In view of the small size of the 65 Mn spring steel sample, the Vickers hardness tester was used for testing. The experimental process strictly implements the national standard GB / T4340.1-2009 [49], the test load is set to 9.8 N, and the holding time is 15 s.

The sample preparation process is as follows: first, the tempered sample is polished on the grinding wheel to obtain a flat test surface; subsequently, the sample was mounted and fixed using a mounting prototype. The inlaid sample is further polished to expose a sufficiently large rectangular area on the front and keep the back flat to meet the requirements of the Vickers hardness test on the surface of the sample. Finally, sandpaper grinding and polishing were used to complete the final preparation.

During the test, in order to reduce the accidental error, three points were randomly selected in the same test surface for measurement, and the average value was used as the surface hardness value of the sample.

2.2.2. Tensile test

The tensile test was carried out on a universal tensile testing machine, and the sample morphology was shown in Figure 2. The experimental conditions were set at room temperature and the stretching speed was 20 mm / min. According to the national standard GB / T228.1-2010, the test is carried out.

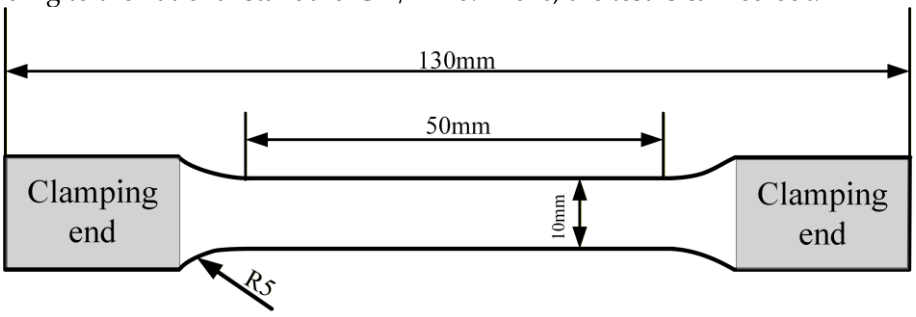

Figure 2. Tensile specimen

Tensile strength is the ratio of the maximum tensile force before fracture to the original cross-sectional area of the sample, which is the key index to evaluate the performance of spring steel wire. In order to analyze the influence of different heat treatment processes on the mechanical properties of 65 Mn steel wire, three parallel samples of steel wire under each process condition were taken for tensile test, and the tensile strength, section shrinkage and elongation were obtained. The average value of the three was used as the mechanical properties of the steel wire under the process.

2.2.3. Torsion test

In this paper, the experiment is carried out according to the national standard GB / T239.1-2012 by using the microcomputer controlled torsion testing machine. The hardness of the test machine chuck is 50-60 HRC, the torsion speed is set to 180 r / min, and the speed fluctuation is not more than 10 %. In the experiment, the two clamps should be strictly coaxial, and the sample should be kept straight to avoid applying bending force.

https://doi.org/10.64486/m.65.3.7

One end of the clamp can rotate freely around the axis of the sample, and the other end only allows axial free movement to ensure that the length change of the sample is not limited. In order to ensure that the sample is straight, the tension force is applied at the free end, and the value is not more than 2 % of the stress corresponding to the nominal tensile strength of the sample. If the fracture of the sample appears in the range of 2 times the diameter from the chuck, the experiment is considered invalid. The final result is the average of three valid experiments.

2.2.4. Bending test

In this paper, the repeated bending test machine is used to evaluate the repeated bending resistance of the material and to reveal its potential defects. The length of the sample is 200-250 mm, which needs to be straightened before the test, and the surface quality should not be damaged. The experiment was carried out in strict accordance with the national standard GB / T238-2002 at room temperature. During the test, the specimen passes through the lever and the clamp, and the lower end is clamped and repeatedly bent at a uniform speed. The bending counting method is as follows: return after bending 90 ° from the starting position to one side, which is counted as the first time; then bend 90 ° to the other side and return, counted as the second time. This was repeated until the specimen was broken, and the total number of bending times (Nb) was recorded. The last bending that caused the fracture was not included. The bending radius of the steel wire will affect the number of bending times, usually the smaller the radius, the less the number of times; as the radius increases, the number of times increases accordingly.

2.2.5. Winding test

The winding test is carried out strictly according to the national standard GB / T2976-2004 ' Metal material wire winding test method ', and the test is completed on the XRC-10 wire winding test machine. The specific method is as follows: one end of the steel wire is fixed on the threaded rod with a diameter of d ~ 3d, and then a bending moment is applied to the steel wire to make it move along the axial direction of the rod (without rotation) and tightly wound. Continue winding until the steel wire breaks, and record the total number of winding turns.

2.3. Microstructure observation

In this study, the microstructure was observed by ZEISS Observer.A1m optical microscope and scanning electron microscope. Before the observation of the optical microscope, the prepared sample is fixed on the glass slide containing the rubber mud by a spring tablet to ensure that the observation surface is parallel to the loading table. During the observation, different areas of the sample were observed and photographed in the order from low magnification to high magnification. In the process, attention should be paid to avoiding direct contact between the lens and the sample. In general, the optical microscope can observe the morphology of the tissue below 500 times, and the model with better performance can be magnified up to 1000 times. In order to observe the fine morphology of specific tissues more clearly, scanning electron microscope is needed.

In this paper, scanning electron microscopy was used to analyze the fracture morphology of the sample and the microstructure of martensite, sorbite and pearlite by selecting 1000 times, 2000 times and 10000 times magnification.

3. Effect of tempering process on microstructure and properties of 65Mn spring steel

3.1. Microstructure analysis

The microstructural evolution of the 65Mn spring steel as a function of tempering temperature is presented in Figure 3. The scale bar in each micrograph corresponds to 50 μm. After tempering at 250 °C (Fig. 1a), the microstructure consists primarily of fine, acicular tempered martensite, characteristic of a low-temperature tempering state. A high density of dislocations is retained within the laths, and very fine carbides are uniformly dispersed, contributing to significant precipitation strengthening. Upon increasing the tempering temperature to 300 °C (Fig. 1b), the martensitic laths begin to widen slightly, and the first stages of carbide coalescence

https://doi.org/10.64486/m.65.3.7

become apparent, indicating the onset of recovery processes. At 400 °C (Fig. 1c), the microstructure shows clear evidence of advanced tempering. The martensite laths have coalesced further, and the carbides have undergone noticeable coarsening and aggregation, leading to a more heterogeneous microstructure with reduced strengthening capability. Finally, after tempering at 500 °C (Fig. 1d), the transformation to tempered sorbitic structure is nearly complete. The carbide particles are significantly coarsened and spheroidized, embedded within a ferritic matrix, resulting in a substantial reduction in dislocation density and overall material softening.

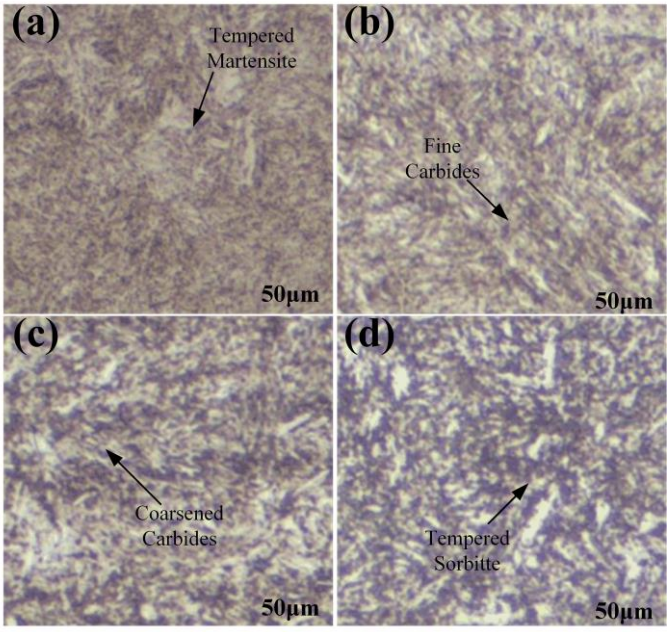

(a)—250 ℃; (b)—300 ℃; (c)—400℃; (d)—500 ℃

Figure 3. Microstructure of the experimental 65Mn spring steel observed at a magnification of 40× after tempering at different temperatures. The key metallurgical constituents, including tempered martensite, fine carbides, coarsened carbides, and tempered sorbitte, are indicated for each condition.

3.2. Mechanical properties analysis

The mechanical properties of the 65Mn steel under different tempering conditions are quantitatively summarized in Table 1. All data points represent the mean value of three tests, with the standard deviation indicating measurement variability. A consistent and strong dependency of all properties on the tempering temperature is observed.

Table 1. Effect of tempering temperature on mechanical properties of 65Mn spring steel (Mean ± SD, n = 3).

Number	1	2	3	4	5	6	7	8
Temperature/℃	250	300	350	400	450	500	550	600
Tensile strength /MPa	2030.5 ± 15.2	1821.8±12.4	1777.1±10.8	1686.2±9.5	1505.7±8.3	1298.2±7.1	1246.6±6.8	1187.1±5.9
Hardness/HV	631±8.5	567±7.2	540±6.8	533±6.5	514±5.9	509±5.7	533±6.1	382±4.2
Section shrinkage /%	36.1±1.2	27.0±1.0	20.9±0.9	18.9±0.8	12.8±0.6	7.9±0.4	5.1±0.3	3.8±0.2
Elongation /%	14.9±0.5	12.9±0.4	11.9±0.4	10.8±0.3	7.9±0.2	7.8±0.2	3.7±0.1	1.8±0.1

https://doi.org/10.64486/m.65.3.7

3.2.1 Hardness

Figure 4 shows the effect of tempering temperature on the hardness of 65Mn spring steel. As a key mechanical property index of materials, hardness can effectively characterize its ability to resist plastic deformation, and is closely related to microstructure and heat treatment process. In this experiment, Vickers hardness tester is used to measure the samples at different tempering temperatures. This method is widely used in the performance evaluation and quality control of metal materials. The results can indirectly reflect the wear resistance, indentation resistance and deformation resistance of materials. With the increase of tempering temperature, the hardness of the experimental steel generally decreases, which is caused by the decomposition of martensite, the precipitation, aggregation and coarsening of carbides, the relaxation of internal stress and the decrease of dislocation density during tempering. When tempered at 250 °C, the hardness reaches the peak value of 631 HV. At this temperature, the fine ε-carbide dispersion distribution produces obvious precipitation strengthening effect, while still retaining a high dislocation density, so that the material has high strength while maintaining good deformation resistance. This hardness peak state well matches the comprehensive requirements of the track and field starter for the high strength and permanent deformation resistance of the elastic element, showing the best engineering applicability.

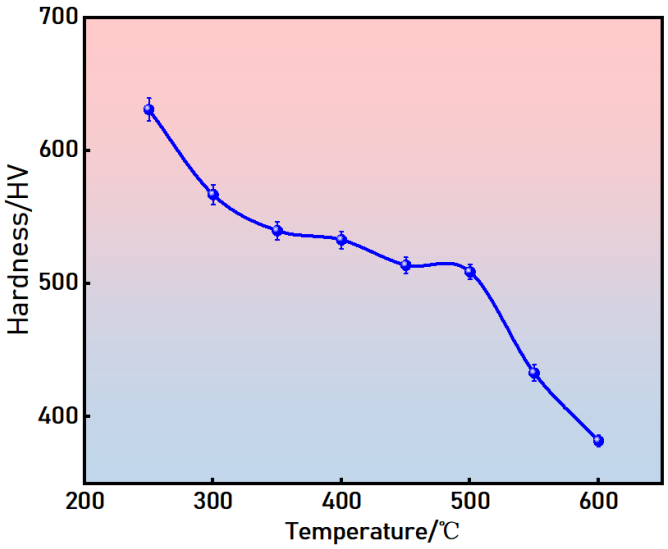

Figure 4. Effect of tempering temperature on hardness of experimental steel

3.2.2 Tensile strength

Figure 5 shows the influence of tempering temperature on the tensile strength of 65 Mn spring steel. Tensile strength, as the maximum stress that the material can withstand before the transition from elastic deformation to plastic deformation until fracture under tensile load, is a key mechanical index to evaluate the strength and toughness of the material. The experimental results show that the tensile strength of the experimental steel decreases monotonously with the increase of tempering temperature. When tempered at 250 °C, the tensile strength reaches a peak value of 2030.5 MPa. This phenomenon is mainly related to the factors such as martensite decomposition, carbide precipitation and aggregation coarsening, internal stress release and dislocation density reduction during tempering. High temperature tempering leads to softening of the structure and coarsening of the strengthening phase, resulting in a significant decrease in strength. Therefore, 250 °C tempering treatment can make the 65Mn spring steel to obtain the optimal tensile properties, suitable for high strength requirements of track and field starter elastic element.

https://doi.org/10.64486/m.65.3.7

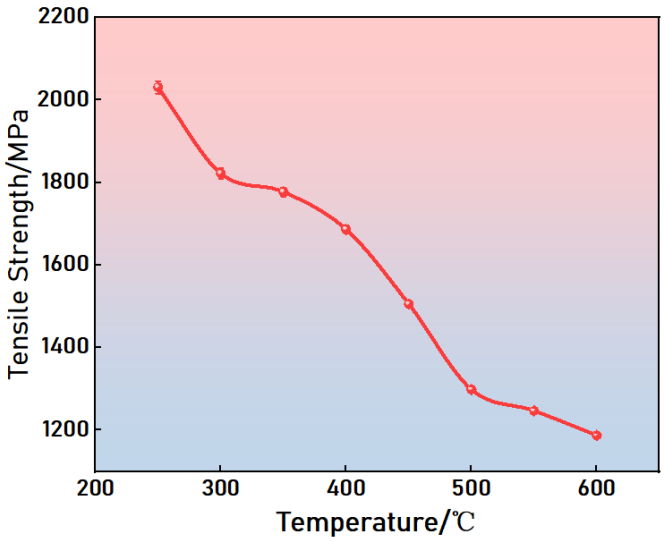

Figure 5. Effect of tempering temperature on tensile strength of experimental steel

3.2.3 Section shrinkage and elongation

The impact of tempering temperature on the plasticity of 65Mn spring steel can be comprehensively understood through the analysis of both the reduction of area and elongation, as depicted in Figures 6. The reduction of area, defined as the percentage decrease in cross-sectional area at fracture relative to the original area in a tensile test, is a critical indicator of a material's ability to undergo plastic deformation and reflects its plasticity and deformation uniformity. Similarly, elongation, which represents the plastic deformation capability of materials before tensile fracture, is another important index reflecting the level of uniform plasticity.

Experimental results indicate that as the tempering temperature increases, both the reduction of area and elongation of 65Mn spring steel exhibit a general downward trend, signifying a gradual decline in plasticity. Specifically, the reduction of area decreases from higher values to a minimum of 3.8 % at 600 °C, while the elongation reaches its maximum of 14.9 % at 250 °C before plummeting to 1.8 % at 600 °C. These trends are intrinsically linked to the evolution of microstructure during the tempering process.

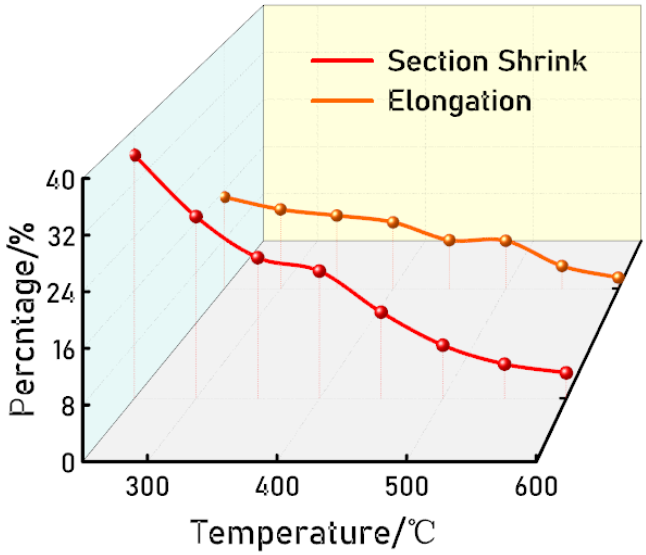

Figure 6. Effect of tempering temperature on section shrinkage and elongation of experimental steel

https://doi.org/10.64486/m.65.3.7

At lower tempering temperatures, the microstructure of 65Mn steel is predominantly composed of fine tempered martensite, which retains a high density of dislocations and fine ε-carbides. This microstructural configuration is conducive to coordinating plastic deformation, thereby maintaining better plasticity. However, as the tempering temperature rises, carbides undergo coarsening and aggregation, martensite decomposition intensifies, and internal stresses are progressively released. These changes lead to a reduction in the material's deformation coordination ability and a significant deterioration of plasticity.

The results underscore that lower tempering temperatures are beneficial for preserving the superior comprehensive mechanical properties of 65Mn steel. This is particularly advantageous for applications requiring high plasticity and toughness, such as elastic components in track and field starters. In contrast, high-temperature tempering is less favorable for scenarios necessitating substantial plastic deformation capacity, as it results in a marked decrease in both reduction of area and elongation. Thus, the selection of tempering temperature is pivotal in tailoring the plasticity and overall performance of 65Mn spring steel for specific engineering applications.

4. Discussion

The mechanical behavior of 65Mn steel is governed by its tempered microstructure. The superior properties at 250 °C are attributed to a fine dispersion of transition carbides (e.g., ε-carbide) within the tempered martensite matrix. Transmission Electron Microscopy (TEM) studies on similar medium-carbon steels confirm that low-temperature tempering (200-300) °C leads to the precipitation of coherent or semi-coherent ε-carbides, which provide strong precipitation strengthening while preserving a high dislocation density [21, 22]. This explains the peak hardness (631 HV) and tensile strength (2030.5 MPa). Importantly, the fine scale of these microstructural features also allows for good deformation coordination, resulting in the retained plasticity (36.1 % RA, 14.9 % EL). This property suite is ideal for a starter component, which requires high strength to resist permanent set and sufficient toughness to absorb impact loads during an athlete's push-off.

As tempering temperature increases, the strengthening carbides coarsen and transform into more stable but less effective cementite (Fe_3C) particles. This coarsening process, along with the recovery of the martensitic matrix and reduction in dislocation density, weakens the precipitation strengthening effect and facilitates easier dislocation motion [23]. Consequently, both strength and hardness decrease. Simultaneously, the coarsened and spheroidized carbides act as less effective barriers to crack propagation and reduce the matrix's ability to undergo uniform plastic deformation, leading to the sharp decline in ductility observed above 300 °C [24]. At temperatures exceeding 500 °C, the formation of coarse, spheroidized cementite in a ferrite matrix (tempered sorbite) results in a soft structure unsuitable for spring applications.

When considering materials for high-performance starter components, a comparison with other spring steels is instructive. For instance, chromium-vanadium steels (e.g., 50CrV4) offer excellent fatigue strength and toughness but often at a higher cost [25]. Silicon-manganese steels (e.g., 60Si2Mn) provide high elastic limit and good hardenability but can be more susceptible to decarburization [26]. The 65Mn steel, treated at 250 °C, presents a compelling balance of very high strength (2030 MPa), good ductility, and cost-effectiveness, which is highly advantageous for the specific loading conditions and economic constraints of sports equipment manufacturing.

5. Conclusions

This study systematically investigated the effect of tempering temperature on the microstructure and mechanical properties of 65Mn spring steel for track and field starters. The results demonstrate that tempering temperature significantly influences the material's properties, with all measured metrics—hardness, tensile strength, reduction of area, and elongation—showing a consistent declining trend as the temperature increased from 250 °C to 600 °C. The optimal comprehensive mechanical properties were achieved at 250 °C, where the material exhibited a peak hardness of 631 HV, a maximum tensile strength of 2030.5 MPa, a reduction of area of 36.1 %, and an elongation of 14.9 %. This superior performance is attributed to the microstructure at this temperature, which consists of fine tempered martensite with a high dislocation density and finely dispersed

https://doi.org/10.64486/m.65.3.7

carbides, providing effective strengthening while maintaining good plasticity. In contrast, higher tempering temperatures led to martensite decomposition, carbide coarsening, and internal stress release, resulting in significant deterioration of mechanical properties. Therefore, the 250 °C tempering process is identified as the optimal parameter, enabling 65Mn spring steel to achieve an ideal balance of high strength, good elasticity, and adequate toughness that meets the performance requirements for elastic components in track and field starters. This finding provides valuable theoretical and experimental basis for material selection and process optimization of this type of sports equipment.

For the track and field starter, the optimal performance of its elastic components is contingent upon a material that synergizes ultra-high strength with adequate toughness. This investigation into the tempering response of 65Mn spring steel for this specific application leads to the following conclusions:

1) Tempering temperature critically controls the microstructure and mechanical properties of 65Mn steel. A consistent decline in hardness, tensile strength, and ductility with increasing temperature is observed, linked to carbide coarsening and matrix recovery.
2) The optimal combination of properties for a starter's elastic component is achieved after tempering at 250 °C for 1 hour. This condition produces a microstructure of fine tempered martensite with a high density of dislocations and finely dispersed transition carbides, resulting in a peak hardness of 631 HV, a tensile strength of 2030.5 MPa, a section shrinkage of 36.1 %, and an elongation of 14.9 %.
3) This optimized 65Mn steel, processed under the 250 °C tempering regime, directly addresses the core mechanical demands of a track and field starter: the exceptional strength prevents permanent deformation of the pedal block under repeated high-impact athlete launches, while the retained ductility provides crucial fracture resistance and durability over extended service. This optimized 65Mn steel offers a competitive balance of high strength, adequate toughness, and cost efficiency compared to other spring steels, making it a suitable and practical choice for the manufacture of durable and high-performance track and field starters.

Acknowledgments: This work was supported by the Jilin Provincial Education Science Leadership Group ' Research on the Development and Supervision Evaluation of Education Internship in Higher Physical Education Institutions ' (Grant No. DD1945).

References

[1] A. G. Ramos et al., "Reliability of the KiSprint force starting block to evaluate different push-off variables in high-level sprinters," Proc. Inst. Mech. Eng., Part P: J. Sports Eng. Technol., vol. 239, no. 2, pp. 170–178, 2025, https://doi.org/10.1177/17543371221110415

[2] F. M. Pérez et al., "A specific test of starting blocks: Intrasession and intersession reliability of isometric strength using a functional electromechanical dynamometer," Appl. Sci., vol. 14, no. 17, Art. no. 7778, 2024, https://doi.org/10.3390/app14177778

[3] I. Matúš et al., "Foot placement in the basic position on the start block OSB12 of young competitive swimmers," Sports, vol. 12, no. 2, Art. no. 42, 2024, https://doi.org/10.3390/sports12020042

[4] M. D. Terjesen et al., "The science of REBT as it relates to performance: Are we in the starting blocks or near the finish line?" J. Rational-Emotive Cogn.-Behav. Ther., vol. 41, no. 2, pp. 272–289, 2023, https://doi.org/10.1007/s10942-023-00500-7

[5] A. M. El Fethi et al., "Impact of mild hypohydration on 100 m front crawl performance and starting block peak force production in competitive university-level swimmers," Sports, vol. 8, no. 10, Art. no. 133, 2020, https://doi.org/10.3390/sports8100133

[6] H. Tong et al., "Microstructure and properties of plasma cladding Fe/Ni–WC gradient composite coating on 65Mn steel," J. Therm. Spray Technol., early access, 2025, https://doi.org/10.1007/s11666-025-02054-9

 https://doi.org/10.64486/m.65.3.7

[7] C. Liu et al., "Effect of bionic scallop microtexture protrusions on the tribological performance of shot-peened 65Mn steel plow surface," Ind. Lubr. Tribol., vol. 77, no. 5, pp. 802–809, 2025, https://doi.org/10.1108/ILT-08-2024-0303

[8] Y. Wan et al., "Effect of Si content and tempering temperature on microstructure and precipitation behavior of graphite particles in Fe–0.58C–1.0Al steel," Int. J. Miner. Metall. Mater., vol. 32, no. 8, pp. 1902–1912, 2025, https://doi.org/10.1007/s12613-025-3115-9

[9] J. N. Ndumia et al., "Microstructure and wear mechanism of FeCrMoCBWNb coating deposited by arc spraying and its application on 65Mn steel blades," Surf. Coat. Technol., vol. 492, Art. no. 131195, 2024, https://doi.org/10.1016/j.surfcoat.2024.131195

[10] Z.-X. Li et al., "Microstructure distribution and bending fracture mechanism of 65Mn steel in laser surface treatment," Mater. Sci. Eng. A, vol. 850, Art. no. 143568, 2022, https://doi.org/10.1016/j.msea.2022.143568

[11] J. Yu et al., "Microstructure and properties of modified layer on the 65Mn steel surface by pulse detonation–plasma technology," J. Mater. Eng. Perform., vol. 31, no. 2, pp. 1562–1572, 2021, https://doi.org/10.1007/s11665-021-06258-2

[12] H. Miao et al., "Mechanical property of U-shaped 65Mn steel bumpers for seismic base isolation," Earthq. Eng. Eng. Vib., vol. 20, no. 3, pp. 791–802, 2021, https://doi.org/10.1007/s11803-021-2052-5

[13] X. W. Su et al., "Mechanical properties of 65Mn chiral structure with three ligaments," Acta Mech. Sin., vol. 35, no. 1, pp. 88–98, 2019, https://doi.org/10.1007/s10409-018-0808-6

[14] H. Xue et al., "Effect of tempering temperature on reheating cracks in the coarse-grained heat-affected zone of 15Cr1Mo1V steel pipe after repair welding," Int. J. Press. Vessels Pip., vol. 218, Art. no. 105590, 2025, https://doi.org/10.1016/j.ijpvp.2025.105590

[15] Y. Huang and G. Zhang, "Microstructure and property of 65Mn steel preheated by laser strengthening," Trans. Chin. Soc. Agric. Eng., vol. 31, no. 1, pp. 53–57, 2015, https://doi.org/10.3969/j.issn.1002-6819.2015.01.008

[16] H. Wang et al., "Effects of boronizing treatment on corrosion resistance of 65Mn steel in two acidic media," Phys. Procedia, vol. 50, pp. 124–130, 2013, https://doi.org/10.1016/j.phpro.2013.11.021

[17] F. R. Wang et al., "Effect of tempering temperature on the microstructure and mechanical properties of Ti-6Al-4V/EH690 clad plates with stainless steel interlayer by vacuum hot rolling," Mater. Sci. Eng. A, vol. 931, Art. no. 148232, 2025, https://doi.org/10.1016/j.msea.2025.148232

[18] C. Dong et al., "Microstructures and properties of electrical discharge strengthened layers on 65Mn steel," Appl. Surf. Sci., vol. 257, no. 7, pp. 2843–2849, 2011, https://doi.org/10.1016/j.apsusc.2010.10.078

[19] A. M. Li and M. J. Hu, "Microstructure and properties of 65Mn steel after austenite inverse phase transformation by sub-temperature quenching," Adv. Mater. Res., vol. 194–196, pp. 89–94, https://doi.org/10.4028/www.scientific.net/AMR.194-196.89

[20] L. Zhu, W. Gao, and Y. Wang, "A self-lubricating composite coating on 6061 aluminum alloy surface with an intermediate anodised layer," Surf. Coat. Technol., vol. 513, Art. no. 132483, 2025, https://doi.org/10.1016/j.surfcoat.2025.132483

 https://doi.org/10.64486/m.65.3.7